

## Drift and diffusion in a periodic two-dimensional velocity field without attractors

F. Müller,<sup>1</sup> L. Schimansky-Geier,<sup>1</sup> V. S. Zykov,<sup>2</sup> and H. Engel<sup>2</sup>

<sup>1</sup>*Institut für Physik, Humboldt-Universität zu Berlin, Newtonstrasse 15, 12489 Berlin, Germany*

<sup>2</sup>*Institut für theoretische Physik, Technische Universität Berlin, Hardenbergstrasse 36, 10623, Germany*

(Received 9 February 2007; published 1 June 2007)

We consider the transport of overdamped particles in a two-dimensional periodic velocity field. This field possesses extended lines of fixed points where the deterministic motion stops. Additive noise makes the lines penetrable and results in an oscillatory motion along tori. We characterize the stochastic motion by the probability distribution density, the stationary mean velocity, and the mean times of escape from bounded domains. For intermediate noise intensities, the fluctuations enhance the transport of the particles compared to the deterministic case. A fast dichotomic modulation of asymmetry enhances fluxes.

DOI: [10.1103/PhysRevE.75.062101](https://doi.org/10.1103/PhysRevE.75.062101)

PACS number(s): 05.40.-a, 47.54.-r, 82.40.Ck

Stochastic methods are powerful tools for describing the transport properties of particles under the action of forces. Examples of Brownian motion in different fields are well known, including free motion, external constant forces, and fields with local minima [1–3]. In particular, Brownian motion in periodic force fields gives examples of phase locking scenarios, while similar methods in the case of nonstationary fields are applied to many variants of ratchets. In many respects the successful description of drift and transport in force fields is caused by the existence of the underlying potential. For one and two dimensions there are many works giving a description of the transport mechanisms in Brownian motors [4–8].

The central dynamics we will investigate has the following structure:

$$\begin{aligned}\dot{x} &=: v_x(x, y) = 2 \sin x \sin y + \eta \cos(x - y), \\ \dot{y} &=: v_y(x, y) = -2 \cos x \sin y + \eta \sin(x - y),\end{aligned}\quad (1)$$

where  $\dot{x}$  and  $\dot{y}$  describe the local velocity components, driven by the two-dimensional velocity field  $\vec{v}=(v_x, v_y)$ , so that no potential can be defined. Equations (1) describe the motion of an overdamped particle where the damping constant is set to 1 by time scale transformation. The only parameter in the system is  $\eta$ . It will be seen that  $\eta \neq 0$  breaks symmetry and an overall motion is induced.

The work we will present here comes from questions arising during the control of spiral wave location in excitable media. This control is important for many applications, including prevention of cardiac arrhythmias [9,10]. In the light-sensitive Belousov-Zhabotinsky reaction [11], the motion of the core of emerging spiral waves can be controlled in different ways [12–14]. The most efficient tool to induce a spiral wave drift is feedback control of the excitability of the medium [15–17]. The feedback signal is proportional to the medium activity integrated over a detector domain, or over several of them. This signal determines the drift velocity field [16–18].

The dynamics of such complex structures can rarely be described by motion in an underlying potential. This field represents a sum of single drift vectors induced separately by each detector domain. With control by two domains, the re-

sulting drift field contains lines of destructive interference [18]. These lines are one-dimensional zones with vanishing velocity ( $v_x=v_y=0$ ) and consist of densely located fixed points. The drift of the spiral core stops at these lines, which therefore act as impermeable barriers in the absence of fluctuations.

The drift velocity field induced far away from a single point detector can be specified as a plane wave  $V_1=\exp[i(x-y)]$ . By construction, the second point generates an orthogonally directed field  $V_2=\exp[i(x+y+\pi)]$ . The velocity field results from the superposition of both,

$$V(x, y) = (1 + \eta) \exp[i(x - y)] - \exp[i(x + y)], \quad (2)$$

where the parameter  $\eta$  determines the difference in the amplitudes. Taking real and imaginary parts, we obtain the two-dimensional velocity field  $\dot{x}=\text{Re } V$  and  $\dot{y}=\text{Im } V$ .

In the case  $\eta=0$ , which we call the symmetric one, lines with an infinite number of fixed points appear at  $y=k\pi$ , where  $k$  is an integer. Along these lines the dynamics is marginally stable. They correspond to regions of vanishing velocity in the  $x$  and  $y$  directions. The remaining nullclines, where one component of the velocity vanishes, are located along  $x=m\pi/2$ . At even  $m$  the velocity in the  $x$  direction disappears, alternating at odd  $m$  with  $\dot{y}=0$  [see Fig. 1(a)]. The  $x$  nullclines possess different stability, which alternates periodically in the two spatial directions. The motion is restricted in cells bounded by fixed point lines and nullclines. Additionally, in the symmetric situation we obtain the parametric phase curves as  $y(x)=-\ln|\sin(x)|+C$  ( $y \neq k\pi$ ), where  $C$  is due to the initial condition.

In the asymmetric case, where  $\eta \neq 0$ , no fixed points exist at all; thus the limitation of the motion disappears and trajectories move along tori. Accordingly, a periodic motion occurs, and trajectories jump in intervals of  $\pi$  in both directions. A sample trajectory starting at  $(\pi/4, \pi/2)$  is shown in Fig. 1(b) for  $\eta=0.1$ .

In the following, due to the periodicity of Eqs. (1), we will focus on the region  $x \in [0, 2\pi]$ ,  $y \in [0, 2\pi]$ , which we call  $\Omega$ .

We compute the integral velocities  $v_x$  and  $v_y$  from integration of the velocity field  $\vec{v}(x, y)$  over the domain  $\Omega$ . They

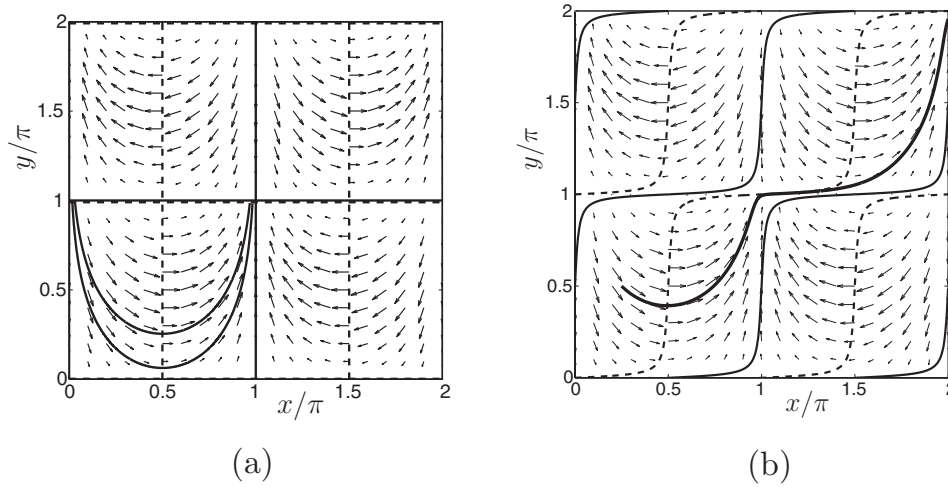


FIG. 1. Velocity field given by Eq. (1) with nullclines ( $\dot{x}=0$ , —;  $\dot{y}=0$ , - - -). The arrows illustrate the direction of the field. (a) Symmetric case ( $\eta=0$ ) with two phase curves; (b) asymmetric ( $\eta=0.1$ ) with a sample trajectory (thick line).

are controlled by the parameter  $\eta$  in the system (1). The velocity in the  $y$  direction is always positive if  $\eta \neq 0$ . In contrast, the sign of  $v_x$  follows the sign of  $\eta$ .

Let us assume that the deterministic dynamics is affected by a stochastic process. We include in Eqs. (1) additional uncorrelated Gaussian white noise with zero mean in the form  $\dot{x} = v_x + \sqrt{2D_x}\xi_1(t)$  and  $\dot{y} = v_y + \sqrt{2D_y}\xi_2(t)$ , where  $\langle \xi_i(t)\xi_j(t+\tau) \rangle = \delta_{ij}\delta(\tau)$  and  $D_{x,y}$  are the noise intensities, respectively. Thus, the particles will be able to cross the fixed point lines by diffusion, and a stepwise propagation in time appears also for  $\eta=0$ . The mean velocity in the positive  $y$  direction becomes nonzero.

In order to study the interaction of drift and diffusion, we investigate the two-dimensional transition probability density  $p(x, y, t | x_0, y_0, t_0)$  and consider the Fokker-Planck equation (FPE) corresponding to the system (1) with additive noise.

First we treat the stationary distribution  $p^0(x, y)$  that develops in the long-time limit, taking periodic boundary

conditions for the region  $\Omega$ . We use the matrix-continued-fraction method [19]. The probability density for  $D_x=D_y=D=0.6$  is shown in Fig. 2(a). It is symmetrically distributed in space for  $\eta=0$ . The parameter  $\eta$  corresponds to the velocity field shown in Fig. 1(a). Although there is no attractor in the system, pronounced accumulation points arise.

However, for  $\eta \neq 0$ , the symmetry is broken, and one direction is preferred as illustrated in Fig. 1(b). In that case also a probability accumulation appears as long as the noise intensities or  $\eta$  are not too large. The maxima are separated by regions of low probability. There are paths of nonvanishing probability, which connect the maxima diagonally. The location of these probability density maxima changes with the noise level. For  $D \rightarrow 0$  they emerge near the fixed point lines. With increasing noise intensity the maxima move down to the deepest sinks of the velocity field, which are located at  $[k\pi, 3(k+2l)\pi/4]$ , with integer  $k$  and  $l$  (see Fig. 3).

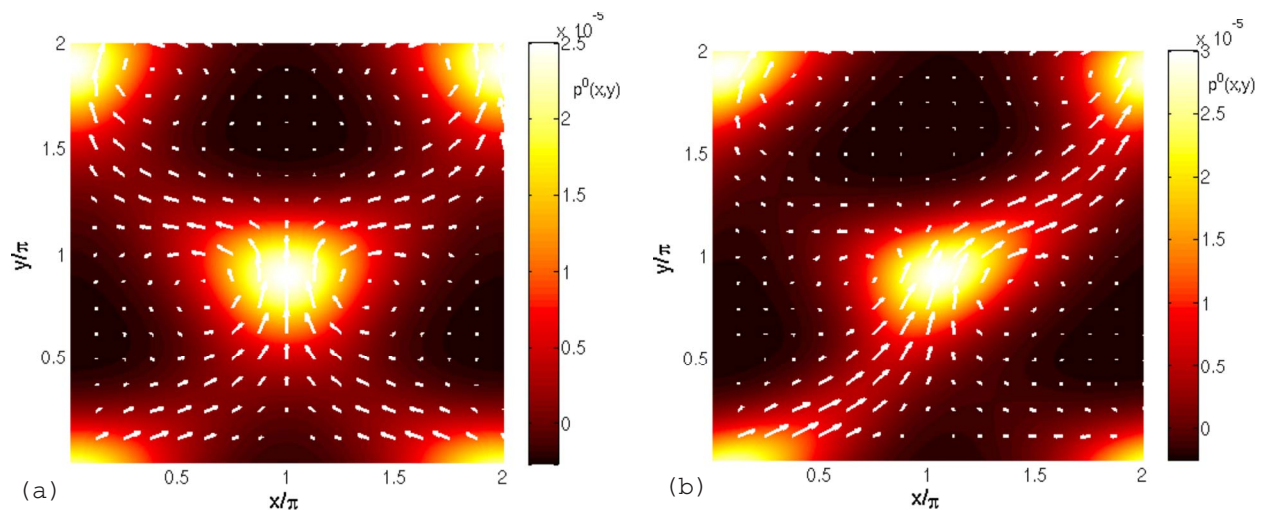


FIG. 2. (Color online) Stationary probability density  $p^0(x, y)$  for  $D_x=D_y=0.6$ . (a) Symmetric,  $\eta=0$ ; (b) asymmetric,  $\eta=0.5$ . The arrows show the vector field of the stationary probability current  $[j_x^0, j_y^0]$ .

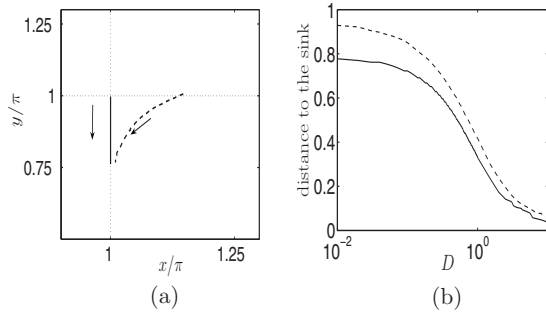


FIG. 3. (a) Location of a probability density maximum in the domain  $\Omega$  with respect to the noise intensity. The arrows show the direction of increasing noise. (b) Pythagorean distance of the maximum to the sink at  $x=\pi$  and  $y=3\pi/4$  versus noise. ( $\eta=0$ , solid line;  $\eta=0.5$ , dashed line.)

The arrows in Fig. 2 indicate the stationary probability current given by  $\partial_t p^0 = -\text{div } \vec{j}^0 = 0$ . Let us consider the integrated currents over the domain  $\Omega$  as

$$J_i^0 = \int_0^{2\pi} \int_0^{2\pi} j_i^0(x,y) dx dy = \langle v_i \rangle, \quad i = x, y. \quad (3)$$

These currents are equal to the mean velocities [8]. Due to the symmetry of the probability distribution, the current in the  $x$  direction disappears regardless of the noise level. If  $\eta \neq 0$ ,  $J_x^0$  decreases monotonically with increasing noise intensity. The solid and dashed curves in Fig. 4 show the noise dependence of the mean  $y$  velocities for  $\eta=0$  and 0.2, respectively. The current in the  $y$  direction reaches the deterministic velocity for small fluctuations, which is finite for  $\eta \neq 0$  and zero for  $\eta=0$ .

At high noise intensities, the  $y$  currents as well as  $J_x^0$  decrease to zero independently of  $\eta$ . In this regime, the probability is asymptotically equally distributed and no directed currents exist. We obtain a maximum for intermediate noise at  $D_{max} \approx 0.64$ , where the current maximizes the transport

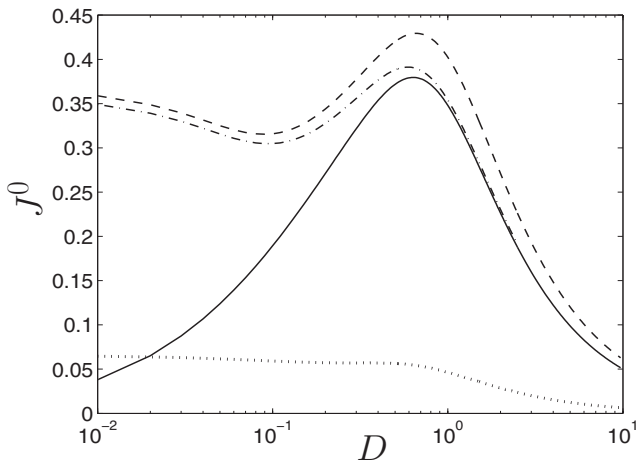


FIG. 4. Integrated stationary probability currents vs. noise intensity.  $J_y^0$  for  $\eta=0$ : solid line,  $J_y^0$  for  $\eta=0.2$ : dashed line,  $\langle J_y^0 \rangle_\eta$  for dichotomously switched  $\eta=\pm 0.2$ : dashed dotted line,  $\langle J_x^0 \rangle_\eta$  for dichotomously switched  $\eta=\pm 0.5$ : dotted line.

through the system. The opposite effect, that the noisy motion is slower than the deterministic one, sets in at noise values about an order of magnitude higher than the local potentials of  $O(1)$  coming from the sinusoidal forces in Eqs. (1).

We stress that the dynamics is not symmetric with respect to a change of the sign of  $\eta$ . The maximum of the  $J_y^0$  current appears inside the interval  $-0.32 \lesssim \eta \lesssim 0.45$ . Outside, the current decrease monotonically.

Dichotomous switching of the sign of  $\eta$  in Eqs. (1) yields surprising effects. Let both signs of  $\eta$  occur with equal probability, so that the mean value of this parameter is zero. First we consider a switching rate that is adiabatically slow. This means that between two switching events the system can reach the steady state. In this case an almost constant net current in the  $x$  direction remains after averaging over both  $\eta$  values. It is shown in Fig. 4 as the dotted curve. This effect is rather small but gets more pronounced for larger  $\eta$ . The corresponding adiabatically switched  $y$  current starts at a finite velocity for  $D \rightarrow 0$  (see dash-dotted line in Fig. 4). For increasing noise level this current approaches asymptotically the curve for  $\eta=0$ , due to the decreasing influence of the asymmetry. On the other hand, at switching rates much faster than the time scale of the dynamics, the currents in both directions are the same as in the fixed symmetric case.

Now we intend to characterize the temporal behavior of the transition probability distribution. A finite difference scheme to solve the FPE numerically is used up to noise intensities of  $D_{x,y} \propto O(10^{-3})$ . To determine the time for the Brownian particle to escape out of  $\Omega$ , we use absorbing boundaries at  $x=y=0$  and  $x=y=2\pi$ .

There are two different time scales in the dynamics of the transition density. One is near the accumulation points, where diffusion plays the dominant role; the other is between them, where the drift governs the dynamics. Near the mentioned maxima of probability the gradient is strong, and therefore the current is large. But the deterministic field is directed opposite to the  $y$  current, there. The preferred way for a particle to leave the accumulation points is diffusion along the fixed point line, until the deterministic velocity field drifts the particle to the boundaries in a relatively short time.

In order to describe such an evolution we use the waiting time distribution  $w(t)$  given by [19]

$$w(t|x_0, y_0) := -\frac{\partial}{\partial t} \int_{\Omega} p(x, y, t|x_0, y_0) d\Omega, \quad (4)$$

and its first moment  $T_{Esc}(x_0, y_0) = \int_0^{\infty} t w(t|x_0, y_0) dt$ , which is the mean time the particle needs to pass the barriers from the chosen initial conditions for a certain noise value and asymmetry.

A comparison of the noisy escape time with the deterministic one with respect to the parameter  $\eta$  is shown in Fig. 5. We choose again  $D_x = D_y = D$  and start at  $x_0 = y_0 = \pi$  with a  $\delta$ -like distribution.

For the symmetric case ( $\eta=0$ ), the purely deterministic escape time  $T_{Esc}(D=0)$  diverges. Increasing noise reduces the escape time monotonically. The drift terms, and accord-

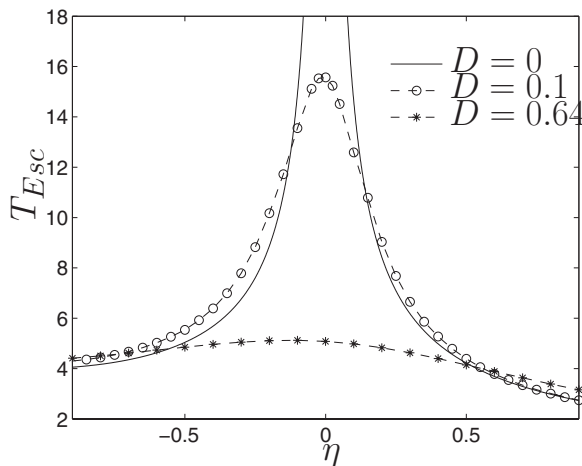


FIG. 5. Escape time with respect to the asymmetry parameter  $\eta$ . The different noise intensities are directed as  $D_x=D_y=D$ . The initial condition is chosen as  $(x_0=\pi, y_0=\pi)$ .

ingly the parameter  $\eta$ , play a less important role, and the curve becomes flat. The more  $|\eta|$  increases for fixed  $D$ , the more the drift governs the motion, the escape takes place with the help of the deterministic velocity, and  $T_{Esc}$  decreases accordingly. However, when  $\eta$  passes a certain value, fluctuations of intermediate strength induce a stabilization for the particle to stay inside  $\Omega$ . Thus the escape times depend on the noise intensity in a nonmonotonic way. For example, for fixed  $\eta \approx -0.3$ , the deterministic escape time is smaller than the one for  $D=0.1$ , but longer than for  $D=0.64$  (see Fig. 5).

We also find parameter regimes for large  $|\eta|$  where the curve with the higher noise value crosses the one with

smaller noise. There the escape times depend on the noise intensities inversely as compared to the mentioned case  $\eta=0$ .

For comparison we solve the two-dimensional diffusion equation without drift terms. We obtain the pure noise escape time as  $T_{esc}^D = \text{const}/D$ , where  $\text{const} \approx 2.91$ , taking the same absorbing boundaries and initial conditions as mentioned before and using Eq. (4). This escape time decreases monotonically with increasing noise as well, but faster than in the symmetric case of the full problem with drift and small noise intensities. In this regime, the pure noise escape time is greater than in the case of the dynamics including drift. From noise intensities of  $D \sim \mathcal{O}(1)$  and above, the behavior of both escape times will be exchanged.

In this work we considered Brownian particles driven by a simple periodic field with particular features. We investigated the Fokker-Planck equation to get the stationary and time-dependent properties of the system, and obtained distinct maxima of accumulated probability density, although there is no attractor in the system. The effect of noise produces a sensitive response of the stationary currents. We found regimes where intermediate noise strength plays a constructive role, entailing enhanced transport through the medium. The transition probability distribution gave us escape times out of the accumulation points, which can be shorter or longer compared to the deterministic motion. Considering a small parameter range, we obtained a complex interplay of drift and diffusion at noise intensities of the order of magnitude of the deterministic force amplitudes.

The authors thank Michael Zaks for constructive discussions and Dirk Hennig for a critical reading of the manuscript.

- 
- [1] B. Lindner, J. Garcia-Ojalvo, A. Neiman, and L. Schimansky-Geier, *Phys. Rep.* **392**, 321 (2004).
  - [2] P. Hänggi, P. Talkner, and M. Borkovec, *Rev. Mod. Phys.* **62**, 251 (1990).
  - [3] I. Sendiña-Nadal, S. Alonso, V. Pérez-Muñuzuri, M. Gómez-Gesteira, V. Pérez-Villar, L. Ramírez-Piscina, J. Casademunt, J. M. Sancho, and F. Sagués, *Phys. Rev. Lett.* **84**, 2734 (2000).
  - [4] H. Gang, A. Daffertshofer, and H. Haken, *Phys. Rev. Lett.* **76**, 4874 (1996).
  - [5] R. Bartussek, P. Hänggi, and J. G. Kissner, *Europhys. Lett.* **28**, 459 (1994).
  - [6] J. Menche and L. Schimansky-Geier, *Phys. Lett.* **28A**, 361 (2001).
  - [7] P. Reimann, *Phys. Rep.* **361**, 57 (2002).
  - [8] M. Kostur and L. Schimansky-Geier, *Phys. Lett. A* **265**, 337 (2004).
  - [9] *Chemical Waves and Patterns*, edited by R. Kapral and K. Showalter (Kluwer, Dordrecht, 1995).
  - [10] V. N. Biktashev and A. Holden, *J. Theor. Biol.*, **169**, 101 (1994).
  - [11] A. N. Zaikin and A. M. Zhabotinsky, *Nature (London)*, **225**, 535 (1970).
  - [12] O. Steinbock, V. S. Zykov, and S. C. Müller, *Nature (London)* **366**, 322 (1993).
  - [13] M. Braune and H. Engel, *Chem. Phys. Lett.* **211**, 534 (1993).
  - [14] V. S. Zykov, A. S. Mikhailov, and S. C. Müller, *Phys. Rev. Lett.* **78**, 3398 (1997).
  - [15] S. Grill, V. S. Zykov, and S. C. Müller, *Phys. Rev. Lett.* **75**, 3368 (1995).
  - [16] V. S. Zykov, G. Bordiougov, H. Brandtstädter, I. Gerdes, and H. Engel, *Phys. Rev. Lett.* **92**, 18304 (2004).
  - [17] V. S. Zykov and H. Engel, *Physica D*, **199**, 243 (2004).
  - [18] V. S. Zykov, H. Brandtstädter, G. Bordiougov, and H. Engel, *Phys. Rev. E* **72**, 065201(R) (2005).
  - [19] H. Risken, *The Fokker-Planck Equation*, 2nd ed. (Springer, Berlin, 1989).